Research Article

Krzysztof Komeza*, Marcin Lefik, Daniel Roger, Ewa Napieralska Juszczak, Hamed Elmadah, Piotr Napieralski, and Noureddine Takorabet

High Temperature Permanent Magnet Synchronous Machine Analysis of Thermal Field

https://doi.org/10.1515/phys-2019-0065
Received May 23, 2019; accepted Jul 18, 2019

Abstract: The subject of the paper is a three-dimensional analysis of a coupled fluid-thermal and electromagnetic field in permanent magnet synchronous machine that can work at very high temperatures. To obtain the distribution of the airflow and temperature we employed the coupled fluid-thermal model of the machine. This allowed us to check whether the temperature in sensitive elements does not exceed the permissible limits. The analysis took into account the effect of the color and the smoothness of the machine housing on the temperature distribution in its interior. The influence of design on the temperature distribution and distribution of hot spots was tested. Two topologies are studied considering magnet mounted on the rotor surface or buried in the rotor soft magnetic core. The simulation results were compared with measurements made on a prototype.

Keywords: Permanent magnet machines, Thermal analysis, Fluid dynamics, High temperature

PACS: 84.50.+d, 47.55.pb, 51.30.+i, 47.27.E-, 07.55.Db, 75.50.Ww

***Corresponding Author: Krzysztof Komeza:** Institute of Mechatronics and Information Systems, Lodz University of Technology, ul. Stefanowskiego 18/22, 90-924 Lodz, Poland; Email: krzysztof.komeza@p.lodz.pl
Marcin Lefik: Institute of Mechatronics and Information Systems, Lodz University of Technology, ul. Stefanowskiego 18/22, 90-924 Lodz, Poland
Daniel Roger, Ewa Napieralska Juszczak: Univ. Artois, EA4025, LSEE, 62400 Bethune France, Technoparc Futura
Hamed Elmadah: Univ. Artois, EA4025, LSEE, 62400 Bethune France, Technoparc Futura; Universite de Lorraine, GREEN Vandoeuvre de Nancy, France
Piotr Napieralski: Institute of Information Technology, Lodz University of Technology, ul. Stefanowskiego 18/22, 90-924 Lodz, Poland
Noureddine Takorabet: Universite de Lorraine, GREEN Vandoeuvre de Nancy, France

1 Introduction

The development of compact electric machines that accept extreme temperatures opens new perspectives for applications of machines in the environment where their use is forbidden until now. These machines will be applied in environments with the ambient temperature which exceeds the typical values. For example, with high temperature (HT°) technologies, machines can be used as compact generators near to the aircraft turbines, where the ambient temperature exceeds 200°C. That can also be use as flexible actuators for many industrial applications as siderurgy or for deep drilling in petroleum industry or in geothermal applications. Of course, as in every electrical machine, the internal losses cause temperature gradients inside the motor housing. The maximum internal temperature can be estimated to 450-500°C at the hottest points of the machine, which are inside the coils. For comparison, the best classical machine made with polymers is limited to an internal temperature of more or less 280°C for a working time of 2000h. Higher temperatures are possible but for shorter times. For high power densities and high ambient temperature, the hottest points of the machine, is much over the capabilities of best polymers that are able to work up to of more or less 240°C during 2000h [1–3]. In order to operate continuously at internal temperatures which are higher than typical, it is required to use inorganic Electrical Insulation System (EIS) and adjust the design of the machine to this technology [4]. The inorganic materials have not the flexibility of polymers. The machine cannot be wound in semi-closed stator slots as it is usually made. The windings must be made of simple-shaped coils which are rigid objects encapsulated with a high temperature cement. Such coils are placed on opened stator teeth and connected together by wires. Consequently, machine windings must be designed with the number of teeth per pole not equal to an integer. The rotor must have many poles. These machines must be synchronous machines or reluctance machines operating at high frequencies. The fractional number of teeth per pole topology requires a specific electromagnetic design for limiting the cogging torque and the

additional losses due to eddy currents. When examining the thermal field distribution, special attention should be paid to sensitive elements. The first element is the temperature of permanent magnets. For this reason, it is necessary to do the design so as not to overheat the magnets. The second element that should be taken into account is the insulation of the coils. To properly track the distribution of hot spots, simulations of the electromagnetic and thermal field should be performed.

For compactness, these machines can be magnetized by permanent magnets in their rotors. They are permanent magnet synchronous machines (PMSM), which have excellent characteristics when they are included in appropriate PWM drives. The paper presents magnetic and thermal analysis of HT° PMSM designed with specific magnets able to work at high temperatures. Two topologies are studied considering magnet mounted on the rotor surface or buried in the rotor soft magnetic core. The influence of the closing the stator slots wedges is also considered.

2 Choice of magnetic materials

The machine's power depends on the energy phenomena which occur in the air gap. These phenomena relate to rotor speed, air gap induction and current density in wires [4]. The first two parameters are related to the quality of mechanical structure of the machine and the magnetic properties of the materials, the third depends on the total heat balance in the engine. If you want to work at much higher temperatures, it is necessary to replace organic insulation by inorganic insulations that do not contain polymers. It should be realized that the mechanical and electrical properties of such insulation differ fundamentally from organic isolation [5]. In the case of windings that work at high temperatures, it is better to use copper for the construction of coils. This is due to the low melting temperature of aluminium and poor electrical properties at high temperatures. As the temperature increases, the conductor undergoes oxidation [6]. To prevent these problems, a cooper is covers with the layer of a protective neutral metal, nickel is the most commonly used material. This additional layer influences the resistance of the wire ant the coil behaviour at high frequencies.

Permanent magnets are the weakest element of a machine designed to work at high temperatures. It is due to the fact that the hight temperature causes the demagnetization of permanent magnets [7–9]. Figures 1 and 2 show the characteristics of different magnets as a function of temperature. Figure 1 clearly shows that standard NdFeB

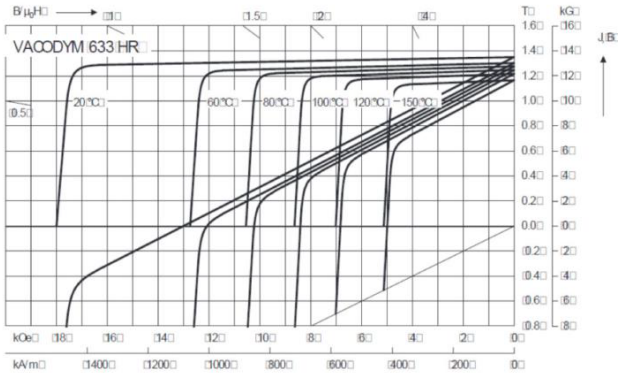

Figure 1: Magnetic characteristic of an example of NdFeB permanent magnet at several temperatures [10].

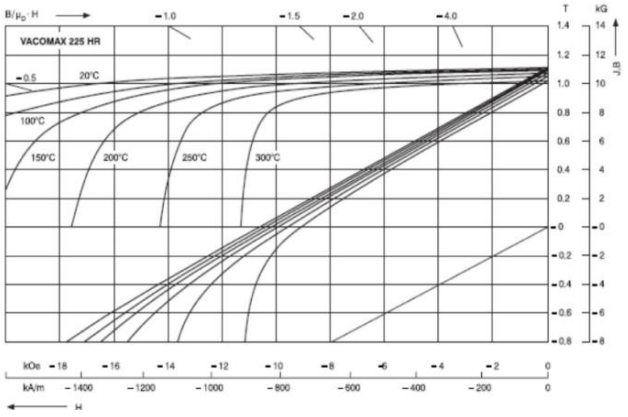

Figure 2: Magnetic characteristic of an example of SmCo permanent magnet at several temperatures [10].

permanent magnets cannot operate above 150°C. The best magnet to operate at higher temperatures is the Samar-Cobalt alloy (shown in Figure 2). These magnets can operate at higher temperatures up to 300°C. In low coercive fields special attention should be paid to designing the magnetic soft core associated with the magnet to avoid large changes in the load lines.

3 General topology of the HT° PMSM

Generally speaking, for PMSM, two rotor topologies are possible: the magnets can be mounted on the surface of the cylinder of soft magnetic material or inside this cylinder. The first option is easier to achieve but it places the magnets near the stator coils. In the second solution the magnets are placed inside the rotor. It caused that the shape of the soft magnetic rotor poles are more complex.

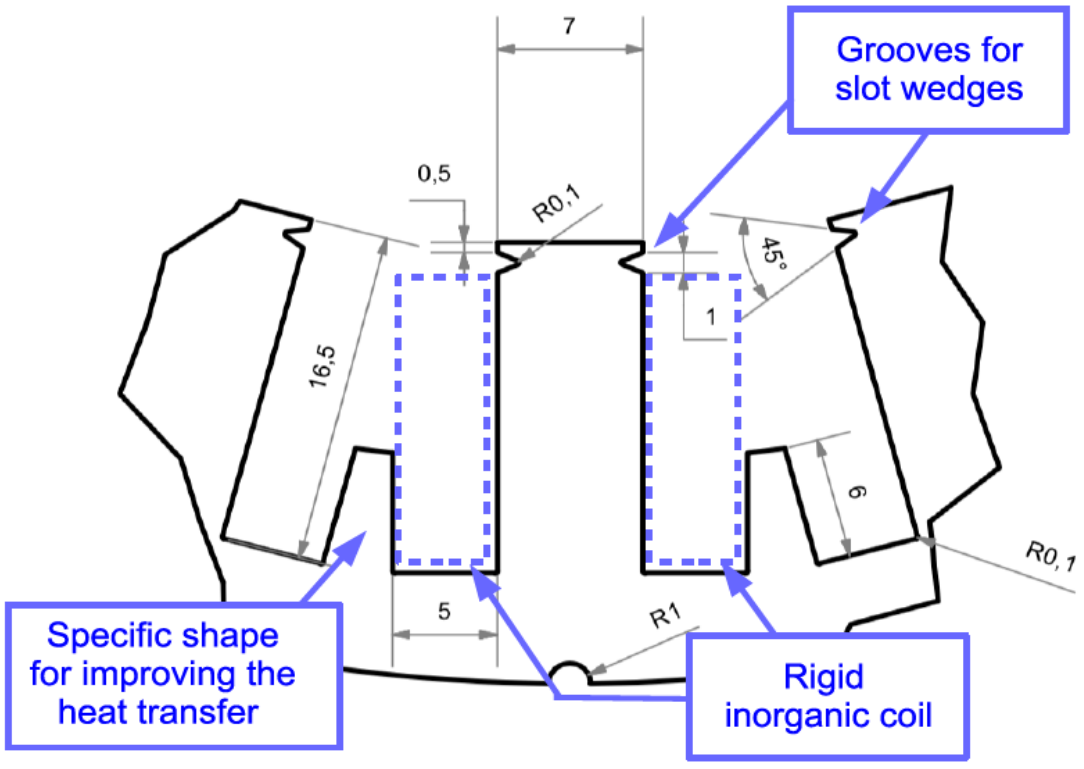

Figure 3: Details of a stator slot designed for a rigid inorganic HT° coil.

Consequently, the magnetic flux is concentrated towards the air gap, and the magnets temperature is lower.

It is important that both variants of the rotors provide an outflow of the heat generated by the eddy current from the magnets.

The two topologies are compared (surface-mounted and interior magnets). Three other options are also considered: the stator slots can be opened (no magnetic wedges - NM) closing the stator slots. The second option considers a stator made with slots closed by wedges made of a composite material (CM) that has a low magnetic permeability, the third option concerns wedges made of magnetic material, most often the one from which the stator is made (MM).

There are several combinations of number of stator teeth and number of rotor poles. The combination 12 teeth / 10 poles is widespread for this kind of machines that operates at lower temperatures. This topology produces an electromotive force with very few harmonics when the machine works as a 3-phase generator and a smooth torque when the machine works as a motor. We opt for this topology but with a duplicate number of teeth and poles (24 teeth and 20 poles), which makes it possible to design a stator core with rectangular teeth that facilitates the mounting of rigid coils. This topology reduces also the height of the stator yoke and consequently facilitates the heat exchanges toward the motor external frame. Figure 3 shows the details of a stator slot designed for a rigid inorganic prefabricated coil.

The first rotor topology using SmCo surface-mounted magnets is presented in Figure 4; the soft magnetic material close the field-lines on the back on the magnets. The mechanical liaison to the central shaft is made by a cross-shaped mechanical steel part. Figure 5 presents details of the second rotor topology where the soft material concentrates the field lines toward the air gap. The mechanical liaison to the shaft is made with a massive non-magnetic stainless steel cylinder, which have external teeth adjusted to the slots between magnets. The details of the mechanical pieces are considered in the general mesh because they influence the thermal transfer toward the shaft.

4 Mathematical Model for thermal analysis

4.1 3D model thermal-fluid coupled

The thermal analysis of the synchronous machine with permanent magnets was carried out using the 3D fluid dynamics calculation (CFD) method. The machine operates

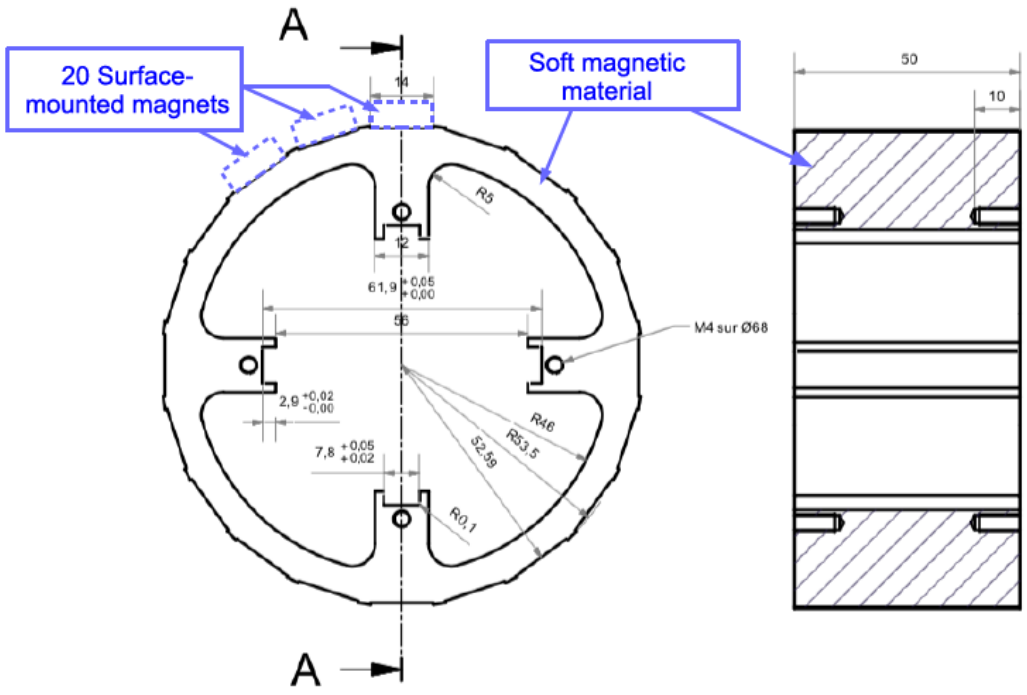

Figure 4: First rotor topology using surface-mounted magnets.

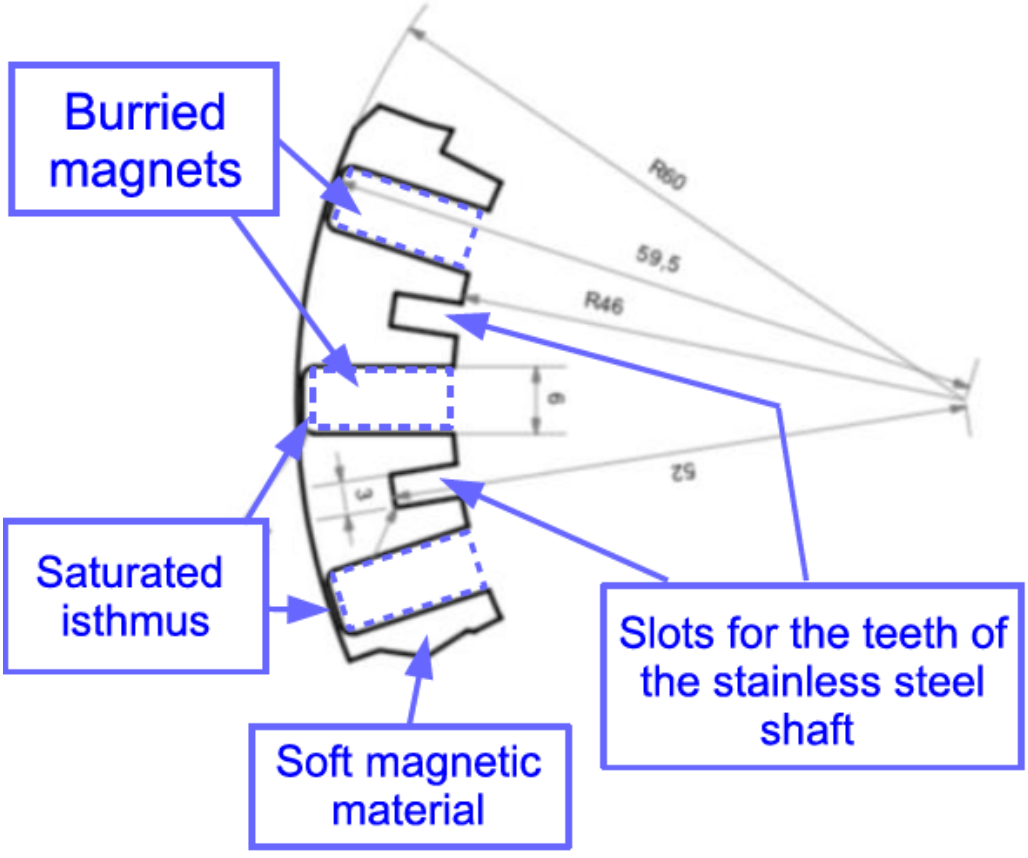

Figure 5: Details of the rotor second topology using interior magnet.

at rated speed of 5650 rpm. The calculations allows to obtain the thermal field distributions inside and outside the machine. The boundary conditions resulting from the condition and colour of the machine surface are taken into account. The influence of the electric conductivity and segmentation of permanent magnets on power losses in magnets and the influence of the materials types on magnetic wedges were tested. This allowed the selection of the optimal design to develop a machine prototype.

The fluid dynamics mathematical model for the turbulent flow of the viscous fluid uses Raynolds-averaged Navier-Stokes equation (RANS model). These equations for the steady state are as follow [13, 14]:

$$\nabla \overline{\boldsymbol{v}} = 0 \tag{1}$$

$$\mu \nabla^2 \overline{\boldsymbol{v}} = \nabla p - \rho \boldsymbol{F} + \nabla \overline{\boldsymbol{\tau}} \tag{2}$$

$$\frac{\lambda}{c\rho} \nabla^2 \overline{T} + \frac{1}{c\rho} \left(\overline{D} + Q \right) - \nabla \overline{\boldsymbol{v} T} - \nabla \overline{\boldsymbol{v}' T'} = 0 \tag{3}$$

where $\overline{\boldsymbol{v}}$ is an averaged values of fluid velocity, $\overline{p}$ is averaged values of fluid pressure, $\overline{T}$ is averaged values of fluid temperature, Q is a heat source density, $\overline{\tau}$ is a Reynolds-stress tensor, $\overline{D}$ is an intensity of dissipation and κ, c, ρ, μ are thermal conductivity, specific heat, mass density and dynamic viscosity respectively.

The RANS model requires turbulence model. It can be k-ϵ model which includes two additional differential equations for the turbulence kinetic energy k and the rate of dissipation of the turbulent energy ϵ [14]. Preparing our model it was necessary to include the rotation of the machine's rotor. It was also important to take into account thermal radiation. These elements have an essential share in the heat transport. The rotation of the rotor can be modelled using the equations of the mobile reference frame, while the other parts of the machine can be modelled using stationary frame equations [14]. An additional phenomenon which should be included in analysis, especially for the HT° machine is radiation. The radiation inside this machine can be calculated with radiation model: Discrete Ordinates or Surface-to-Surface. For external walls of the machine the radiation phenomenon can be included by the mixed boundary condition for energy equation (2) are used. Combined boundary condition is given by following formula [15]:

$$-\kappa \frac{\partial T}{\partial n} = h_c \left(T_w - T_\infty \right) + \varepsilon_r \sigma \left({T_w}^4 - {T_{ext}}^4 \right) \tag{4}$$

where h_c is a convective heat transfer coefficient, T_∞ is temperature of the ambient air, T_w is surface temperature of the wall, T_{ext} is the ambient temperature, ϵ_r is the surface coefficient and σ is the Stefan-Boltzmann constant. The convective heat transfer coefficient h_c can be determined from empirical formula which is based on dimensionless Rayleigh and Nusselt numbers.

Three-dimensional coupled thermal-fluid model of the HT° machine is prepared using commercial Ansys Fluent package. This model includes all parts of the machine also shaft, housing and bearings. It is necessary to include all elements participate to the heat transport in the machine. Two variants of HT° machine was analysed: with surface-mounted permanent magnets and second with the magnets buried into the rotor. Solid models with finite volume mesh of both machine variants are shown in Figure 6. The finite volume mesh of the whole HT° machine is large: more or less over 7 million elements for the machine with surface-mounted magnets in the rotor and 9 million elements for the machine with buried magnets. The sources of the heat in the model of the HT° machine are power losses obtained from electromagnetic analysis.

4.2 Estimation of local losses by electromagnetic simulations

To calculate the losses and distribution of the electromagnetic field the simulation program Opera was applied, considering the machine working as a synchronous generator. An external motor drives the shaft at 5000 rpm. The stator phases are connected to load resistances for getting a stator current of 4 A at 833 Hz. First the 2D simulations were performed for computing core losses with a reasonable computing time. The time-stepping analysis was performed over approximately 20 electrical periods for waiting the steady state; then, the induction components B_x and B_y were recorded at regular short intervals (800 times per period). A macro was developed for calculating losses in the stator and rotor soft core using Discrete Fourier Transform (DFT) of the recorded data [16, 17]. With such a large number of samples per period, the core losses were computed considering slots effects. The details of DFT computations are given by (5) and (6). In these expressions N is the number of sample (N=800) and k the rank of the harmonic (0…400), according to the Nyquist–Shannon sampling theorem.

$$B_{xk} = \sum_{n=0}^{N-1} B_x(n)\, e^{-i2\pi k/N} \tag{5}$$

$$B_{yk} = \sum_{n=0}^{N-1} B_y(n)\, e^{-i2\pi k/N} \tag{6}$$

(a)

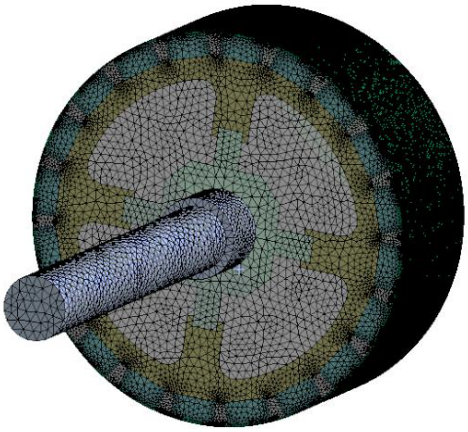

(b)

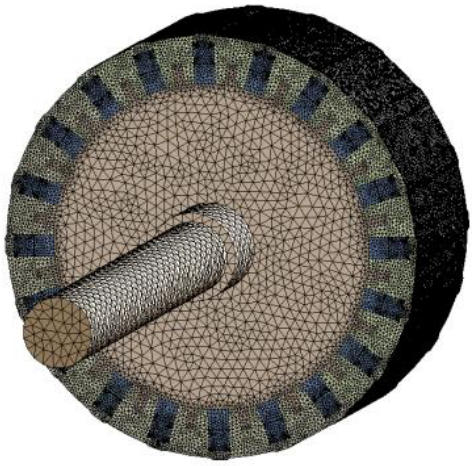

(c)

Figure 6: Model of machine with volume element mesh: a) Stator identical for both rotors; b) rotor with surface-mounted magnet, c) rotor with interior magnets.

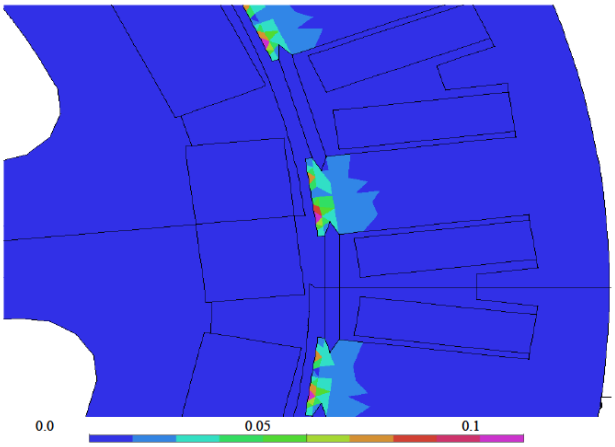

Figure 7: Distribution of 5th harmonic magnitude of magnetic flux density [T].

The calculation of losses necessitated extrapolation of the specific loss characteristic of the material for frequencies above 5000Hz. The iron loss model is based on loss separation. This extrapolation used the measured values in the range 50-5000Hz and had the form of eqn. (8) where w_{Fe} is the power density inside the core $[W/m^3]$, f is the frequency $[Hz]$, B flux density magnitude $[T]$. The method of calculating the approximation factors based on the results of the measurement of material properties is described in [17]. For this extrapolation method measurements were carried out on a large diameter toroid sample, which yields a very high uniformity of magnetic field strength inside the sample. The values the maximum flux density, power loss, maximum magnetic field strength in the core was determined. For the Vacoflux 48, the coefficient estimation are $k_e = 1.36\ 10^{-5}$ $k_h = 2.223\ 10^{-2}$, $\alpha = 2.726$ and $\beta = 1.147$. k_e is the coefficient concerning the eddy current losses and k_h the hysteresis losses.

$$w_{Fe} = k_e f^2 B^{\alpha} + k_h f B^{\beta} \tag{7}$$

Based on the two component of the flux density given by (5) and (6), the program calculates iron losses with (7) for each harmonics. Figure 7 gives an example of distribution of 5^{th} harmonic magnitude of magnetic flux density in the magnetic core. As expected, the flux density and losses concentrate in part of the teeth close to the air-gap, where the flux density variations are the largest during the rotation. (the induction is less than for the 1 harmonic but the frequency is higher)

The winding losses are calculated for each stator coils from their resistances and the RMS phase current computed in steady state by the electric circuit of the 2D model.

For calculating losses distribution inside permanent magnets and slot wedges, it is necessary to use a 3D sim-

ulation because these losses results mainly of eddy currents, which have a dominant axial component. The 3D mesh contains about 4.26 million elements for the whole machine. Magnetic vector potential formulation with linear edge elements was used in that analysis. The analysis relies upon a remeshing technique. During the transient analysis, before the solution at the next time-step, the position of each moving part is updated. In conducting material as magnet and wedges, the element sizes must be under one-third of the estimates skin depth. With such a large 3D mesh, the computation time become very large, for getting results in reasonable delays, the simulations were performed for a quarter of the machine with a virtual computer made of eight cores. Figure 8 is an example of such results; it gives an image of eddy currents in magnets. The losses are computed by (8) from the current density magnitude J $[A/m^2]$; $w_c$is the power density $[W/m^3]$ in the conducting material (magnet or wedge), σ the material conductivity $[S/m]$.

$$w_c = \frac{1}{\sigma} J^2 \tag{8}$$

Figure 8 presents an example of the distribution of eddy currents on the surface; the influence of the stator teeth can be observed.

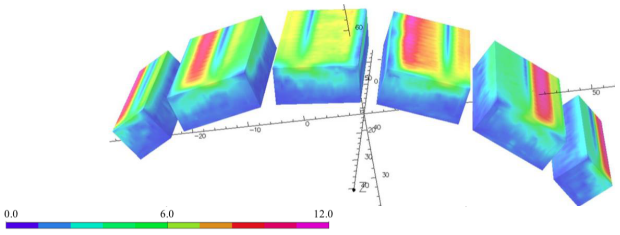

Figure 8: Current density distribution [A/mm^2] on the surface of PM.

The distribution the losses density $[W/m^3]$ in each part of the machine is the input data of the thermal-fluidic model that computes the temperatures. The average loses in each parts presented in Table 1 are obtained by volume integration. (all losses are the total losses for the whole machine, the effective length of the machine was 50 mm)

5 Results of the thermal numerical analysis

The coupled thermal-fluid and electromagnetic models are able to compute the temperature distributions outside and inside the machine. A series of simulations concerning different designs were made: for surface-mounted magnets and interior magnets for an ambient temperature of 200°C. These models were used to verify influence of wedge closing the slots of stator on the temperature distribution.

Table 1: Total losses in the main elements.

Machine part	Total losses for the machine with surface magnets [W]	Total losses for the machine with interior magnets[W]
Stator	68,9	54,7
Rotor	34,87	27,8
Coils	499,2	499,2

5.1 Effect of wedges made from magnetic material on the temperature distribution

The use of wedges affects a number of machine properties. Among other things, it limits losses, as well as limits cogging torque. It should be realized that when using metallic wedges, eddy currents are induced in them. This will increase the losses from the eddy currents and create a hot points in the wedges and near the wedges. It is necessary to test different types of wedges, both magnetic and non-magnetic, as well as the functioning of the machine without wedges, in order to correctly choose a prototype.

The following assumptions are included in the analysis:

- the radiation phenomena and the air-flow inside the machine's housing are take into account,
- the power losses in the rotor for the variant with the internal magnets with the wedges and without the wedges are the same,
- power losses for variants with surface magnets and interior magnets have been calculated in the manner described in the previous paragraph.

It has been observed that the power losses for variant with surface mounted magnets without wedges are greater than for variant without wedges. It is assumed that for variant with surface mounted magnets (with wedges and without them), the power losses will be equal for losses for variant with interior magnets (with wedges and without them). On the Figure 9 for the rotor with interior magnets and stator slots with magnetic wedges (Figure 9a); for rotor with interior magnets and stator slots without wedges (Figure 9b). In turn, Figure 10 shows the temperature distribution in the rotor for two cases: the first for slots of stator

Table 2: Total losses in wedges and magnets.

Total power in elements [W]	Stator with wedges		Stator without wedge	
	Surface magnets	Interior magnets	Surface magnets	Interior magnets
Permanent magnet	22,9	0,72	34	1,07
Wedges	153,3	153,3	-	-

Table 3: Temperatures for selected machine parts for both variants.

Motor part	Surface-magnet with wedge °C	Surface-magnet without wedge °C	Interior-magnet with wedge °C	Interior-magnet without wedge °C
Magnets	307	283	281	240
Wedges	321*	271**	300*	246**
Rotor core	305	281	281,4	240
Stator core	307,0	266,6	288,6	245,9
Winding	312,6	273,1	293,6	250,0
Housing	236,5		221,3	

* - magnetic wedge; ** - non-magnetic wedge

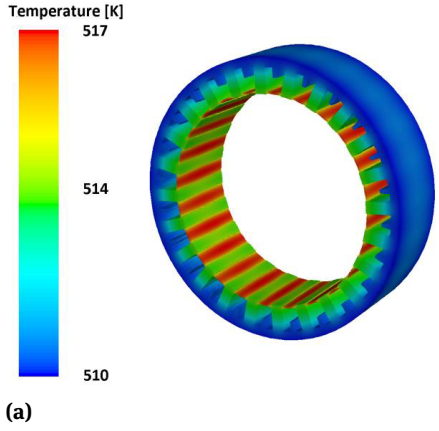

Figure 9: The temperature distribution on the stator surface: a) rotor with interior magnets and stator slots with wedges, b) rotor with interior magnets and stator slots without wedges.

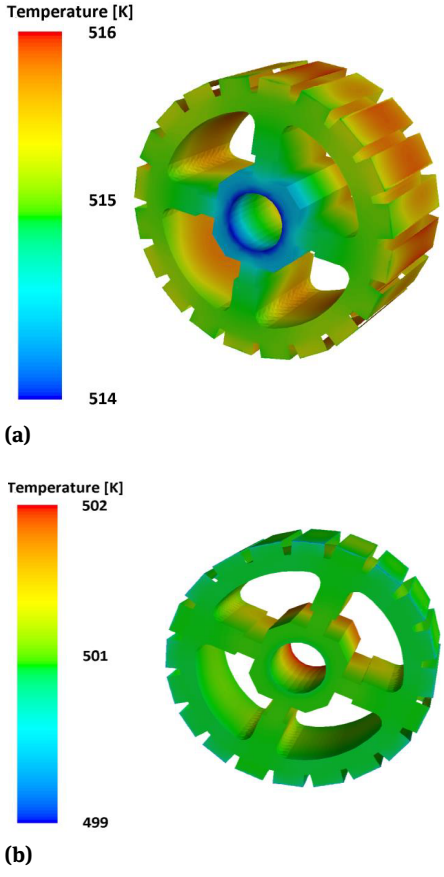

Figure 10: The temperature distribution on rotor with surface-mounted magnets: a) stator slots with wedges, b) stator slots with without wedges.

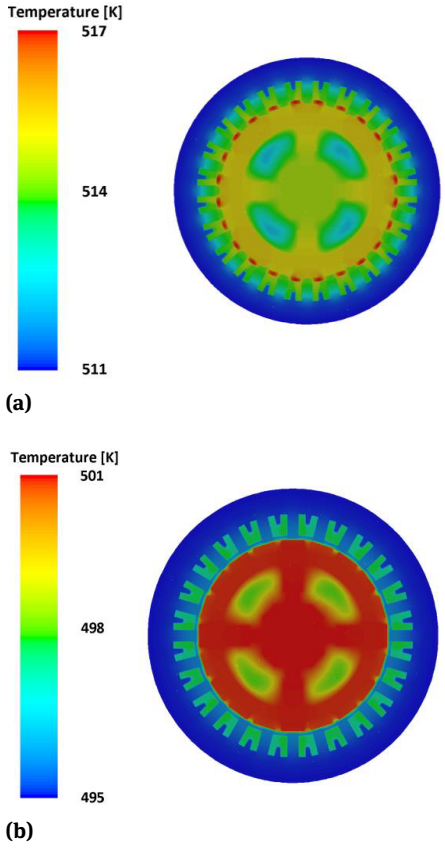

Figure 11: Temperature distribution in the motor cross-section XY: a) rotor with surface-mounted magnets and stator slots with wedges, b) rotor with surface-mounted magnets and stator slots without wedges.

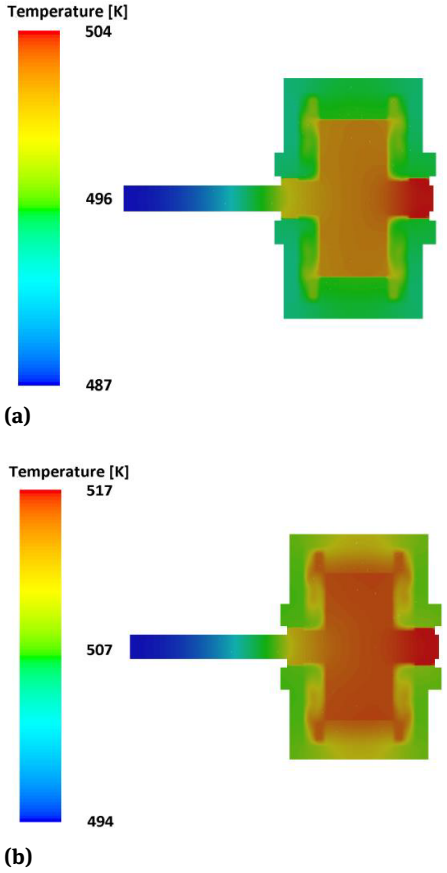

Figure 12: Temperature distribution in the motor cross-section XZ: a) rotor with surface-mounted magnets and stator slots with wedges. b) rotor with surface-mounted magnets and stator slots without wedges.

closed with magnetic wedges, the second without the use of wedges.

Figure 11 shows the temperature distribution in the motor cross-section XY, and Figure 12 for the cross-section XZ.

Figures 12 and 13 allow comparisons of the temperature distribution for both variants (with surface magnets and interior ones; for the stator case with wedges and without wedges), which allowed to infer conclusions about the effect of design and wedges material on the heat distribution in the machine and the existence of hot spots.

The results of calculations are shown in the Table 3. This table presented the mean values of temperatures in selected parts of the machine for both analysed variants and versions (with and without wedges).

Figure 14 shows the temperature distribution at the outer surface of the housing for an ambient temperature of 200°C.

As we can see the use of magnetic wedges allows to reduce the power loss for the variant with interior magnets. The only reasonable structure is therefore the permanent magnet synchronous machine in which the magnets made of SmCo alloys are built into the core of the rotor. From a magnetic point of view, the technological lock is located at the level of the magnets. The samarium and cobalt alloys, they have interesting properties up to 340°C, but without the possibility of leaching PMSM control.

6 Application of results

The temperature maps produced by the thermal model show that the magnetic wedges that close the stator slots are the hottest point of the machine. The stator wedges have a very important positive effect on the cogging torque but a negative one on the machine thermal management. Without wedges, the hottest points are inside the stator coils, near the air-gap. For both cases, with an ambient temperature of 200°C the coils must withstand temper-

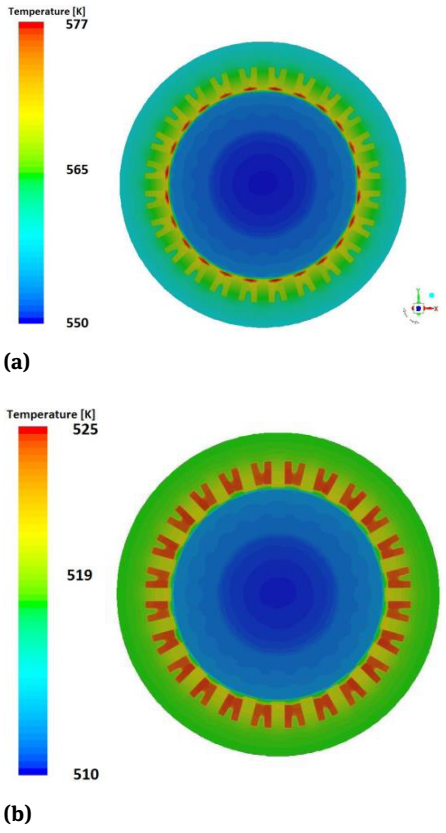

Figure 13: The temperature distribution in the motor - cross section XY: a) rotor with interior magnets and stator slots with wedges, b) rotor with interior magnets and stator slots without wedges.

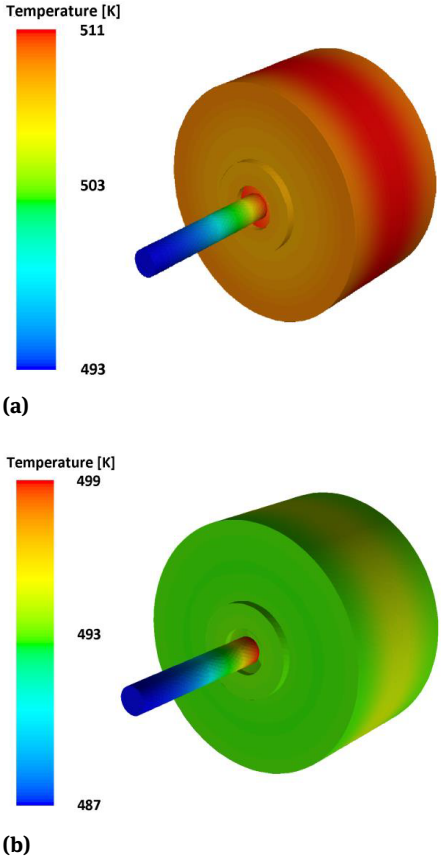

Figure 14: The temperature distributions outside HT machines: a) variant 1 with wedges, b) variant 1 without wedges

atures over the classical polymer technologies capabilities. Another coil technology has been developed with a fully inorganic electric insulation system (EIS) and copper wires protected against oxidation by a thin nickel layer. The wire is embedded in high temperature cement based on alumina and other inorganic specific materials that yield the adequate crystalline structure during the hardening thermal cycles. With the developed building process and the correct thermal cycles made in a stainless still mould, the new inorganic coils are rigid objects with very hard surfaces and a correct resistance to repetitive shocks [15]. They are able withstand very high temperatures, up to 500°C without any mechanical damage. However, the HT° cement is a porous material at the micrometre scale. This drawback limits the electrical breakdown voltage. Figure 15 illustrate this property; it gives the partial discharge inception voltage PDIV and the breakdown voltage of the turn-to-turn insulation for several temperatures up to 500°C for two set of inorganic wire of diameter 0.5mm and 0.8mm [16]. Let us remind that, for such wire diameters, the classical organic coil have a PDIV in the range of 700-800V and a much higher breakdown voltage.

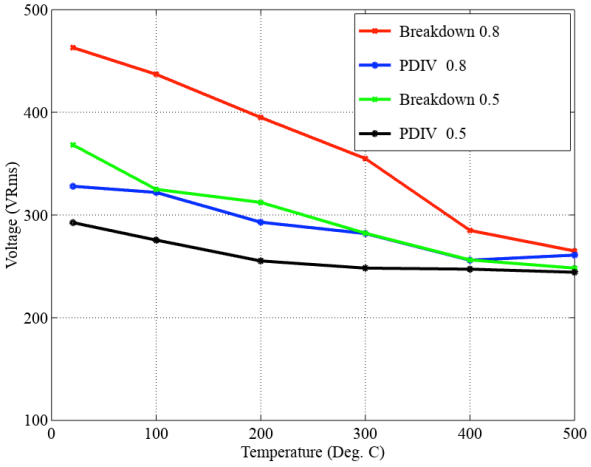

Figure 15: Partial Discharge Inception voltage (PDIV) and breakdown voltage of the inorganic coil turn-to-turn voltage for two wire diameters (0.5mm and 0.8mm).

With lower electrical performances, inorganic coils must be designed with a special care for limiting the turn-to-turn voltage. Figure 16 gives an example of design able to get a low turn-to-turn voltage. This 16-turn coil corre-

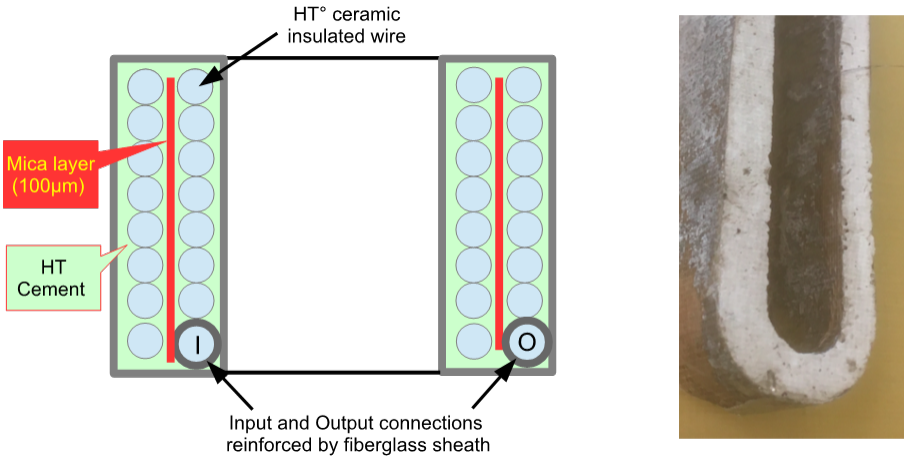

Figure 16: Example of a HT° coil design able to operate continuously at temperatures computed by the thermal model.

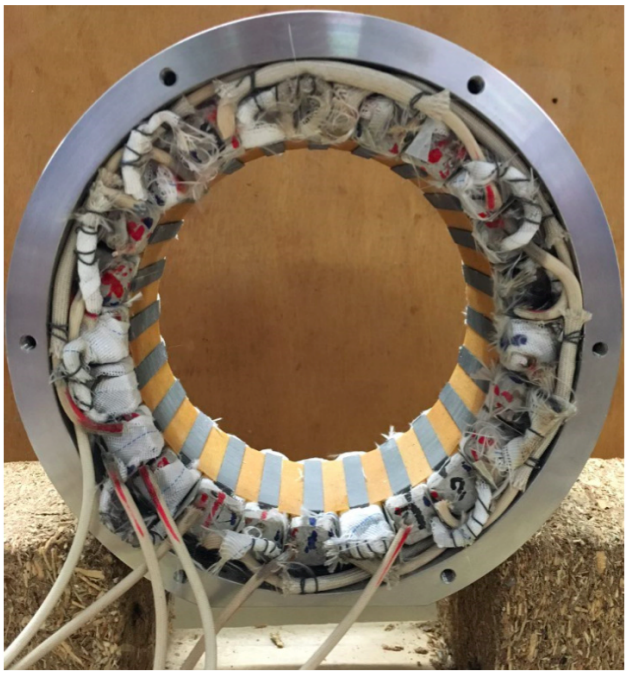

Figure 17: 24-tooth stator made with inorganic HT° coils able to operate up to 500°C.

sponds to the design of a 5000 rpm 24-tooth 20-pole permanent magnet synchronous machine. This coil can withstand transient voltage pulses produced by a PWM inverter connected to the standard 540 volts dc bus. The two-layer separated by a thin mica film, able to operate over 500°C, reinforces the layer-to-layer insulation. With such a turn distribution the turn-to-turn voltage remains much under the PVIV at 500°C for the highest voltage short spikes applied to the machine. Figure 16 presents a cross section of the coil and a detail of its external hard surface lade of cement. Figure 17 shows the whole 24-tooh HT° stator.

7 Conclusion

The subject of our work was the analysis of the possibilities of working asynchronous machine with permanent magnets in a high temperature environment. We found that at an outdoor temperature of 200°C, the temperature around coils and permanent magnets can exceed even 400°C. In the study, we focused particular attention on the phenomena in the insulation of coils and the selection of permanent magnets.

We found the following facts:

- If the temperature of the coils exceeds 300°C, it is necessary to replace the organic insulation by inorganic insulation,
- Inorganic insulation is rigid, which requires proper machine design. It demand the use of rectangular teeth and open slots,
- Only one coil is placed on each tooth,
- With this structure, the eddy currents and losses in the machine are larger,
- At such a high temperature, it is necessary to use SmCo permanent magnets. This type of magnet is characterized by high conductivity,
- We checked various design possibilities and found that it is necessary to segment the magnets and close the stator's slots by wedges,
- We analyzed the effect of different types of wedges on the temperature distribution and on the value of hot spots in magnets and coils. We stated that the best results give the use of martensinite steel with low magnetic permeability,

- Despite the occurrence of losses from eddy currents in wedges, total losses are definitely lower than in machines without wedges,
- Best results for both temperature and cogging torque were obtained for the construction with embedded magnets,
- The machine with permanent magnets can be used for temperatures below 350° C, for higher temperatures it is necessary to use a reluctance machine with inorganic coil insulation.

References

[1] Ho J., Jow T., Effect of crystallinity and morphology on dielectric properties of peek at elevated temperature, 2013 IEEE International Conference on Solid Dielectrics (ICSD), June 2013, 385–388

[2] Hoang A. T. T., Serdyuk Y. V. V., Gubanski S. M. M., Electrical characterization of a new enamel insulation, IEEE Transactions on Dielectrics and Electrical Insulation, 2014, 21, 3, 1291–1301

[3] Raminosoa T., E-Refaie A. M., Torrey D. A., Grace K., Pan D., Grubic S., et al., Test Results for a High Temperature Non-Permanent-Magnet Traction Motor, Industry Applications IEEE Transactions on, 2017, 53, 4, 3496-3504

[4] Iosif V., Roger D., Duchesne S., Malec D., An insulation solution for coils of high temperature motors (500°C), 2016 IEEE International Conference on Dielectrics (ICD), August 2016, 1, 297 – 300

[5] Fothergill J., Ageing, space charge and nanodielectrics: Ten things we don't know about dielectrics, in Solid Dielectrics, ICSD'07 IEEE International Conference on, July 2007, 1–10

[6] Malec D., Bley V., Lebey T.,Investigations on dielectric breakdown of ceramic materials, in Electrical Insulation and Dielectric Phenomena, 2005. CEIDP'05, 2005 Annual Report Conference on, October 2005, 63–66

[7] Zhu K., Mimura Z., Isshiki M., Oxidation Mechanism of Copper at 623-1073K, Japan institute of metals, 2002

[8] Takahashi N., Morishita M., Miyagi D., Nakano M., Examination of magnetic properties of magnetic materials at high temperature using a ring specimen, Magnetics, IEEE Transactions on, 2010, 46, 2, 548–551

[9] Cozonac D., Lecointe J.-P., Duchesne S., Velu G., Materials characterization and geometry of a high temperature induction machine, in Electrical Machines (ICEM), 2014 International Conference on, Sept 2014, 2499–2505

[10] Liu J., Walmer M., Thermal stability and performance data for SmCo 2:17 high-temperature magnets on ppm focusing structures, IEEE Transactions on Electron Devices, 52, 5, 899–902

[11] Advanced materials – the key to progress, Vacuumschmelze, https://www.vacuumschmelze.com/fileadmin/Medienbiliothek_2010

[12] Iosif V., Roger D., Duchesne S., Malec D., Assessment and improvements of inorganic insulation for high temperature low voltage motors, IEEE Transactions on Dielectrics and Electrical Insulation, 2016, 23, 5, 2534–2542

[13] Gryboś R., Fundamentals of fluid dynamics. Part 1, Warszawa, PWN, 1998, (in Polish)

[14] Melka B., Smolka J., Bulinski Z., Ryf A., Hetmanczyk J., Makiela D., A Validated Numerical Model of Heat and Mass Transfer in a PM BLDC Electric Motor, August 2016, International Symposium on Power Electronics, Electrical Drives, Automation and Motion (SPEEDAM)

[15] ANSYS® Academic Research, Release 17.2, Help System, Theory Guide, ANSYS, Inc.

[16] Komeza K., Napieralska Juszczak E., Roger D., Takorabet N., Meibody-Tabar F., Lefik M., Analysis of the Impact of the Design of HT Machines on the Cogging Torque and Losses in Permanent Magnets, December 2016, IEEE International Conference on Power Electronics, Drives and Energy Systems IEEE PEDES 2016

[17] Komeza K., Dems M., Szulakowski J., Kubiak W., Modeling of core loss for non-oriented electrical steel, June 2018 International Symposium EPNC